



International Congress of Science and Technology of Metallurgy and Materials, SAM –  
CONAMET 2014

## Zinc + nickel + microparticles coatings: production process and structural characterization

Zulema A. Mahmud<sup>a,\*</sup>, Franco Amelotti<sup>a</sup>, Carlos Serpi<sup>a</sup>, Jorge Maskaric<sup>b</sup>, Martín Mirabal<sup>b</sup>, Norma Mingolo<sup>c</sup>, Liliana Gassa<sup>d</sup>, Paulo Tulio<sup>e</sup>, Gabriel Gordillo<sup>f</sup>

<sup>a</sup>INTI, Av. Gral Paz 5445 Procesos Superficiales Ed 46. CC 157-1650 San Martín. Argentina

<sup>b</sup>Dropur S.A. L N Alem 3560, Munro, Buenos Aires, Argentina

<sup>c</sup>CNEA. Comisión Nacional de Energía Atómica, Buenos Aires, Argentina

<sup>d</sup>Instituto de Investigaciones Físicoquímicas Teóricas y Aplicadas, INIFTA, UNLP, Argentina

<sup>e</sup>Univ. Tecnológica Federal do Paraná UTFPR/PR, Brazil

<sup>f</sup>Facultad de Ciencias Exactas y Naturales, UBA, Argentina

### Abstract

The properties of coatings obtained from Ni-Zn electrodeposition baths containing microparticles is analyzed. The incorporation of alumina or silicon carbide microparticles improves properties of hardness and protection of the coating. The Ni content in the alloy, which normally varies between 10 and 15 %, was measured by X-ray fluorescence. ZnNi-particles coatings show a high nickel content and high corrosion resistance. The incorporation of uniformly distributed particles in the coatings is achieved under controlled conditions of current density and mechanical stirring. It was found that in the present case, 8 A/dm<sup>2</sup> is the optimal electrodeposition current density. Frontal coatings samples were studied by scanning electron microscope while cross sectional area by optical microscope. The surface analysis was performed by energy dispersive X-rays spectroscopy microprobe and the structural characterization by X-ray diffraction. The last technique showed that the phase (3,3,0) is reinforced after 10 minutes of electrodeposition in the presence of CSi, while there is a change from ZnNi (3,3,0) to ZnNi (1,1,0) in the presence of Al<sub>2</sub>O<sub>3</sub>. This led to an increment of the compressive forces in the material. The charge transfer resistance (RTC) of the coating depended on its own thickness. High values of RTC corresponded to lower values of corrosion current J<sub>0</sub>. Experimental results showed that  $RTC_{10\text{ microns}} > RTC_{20\text{ microns}} > RTC_{5\text{ microns}}$ , indicating that the best properties of the material were obtained at 10 microns. In industrial scale process and in the laboratory, it was found that electrolyzing during 10 minutes with different J is:  $RTC(8\text{ A dm}^{-2}) > RTC(10\text{ A dm}^{-2}) > RTC(6\text{ A dm}^{-2})$ . Zn-Ni-CSi coatings showed a decrease in the crystal size when saccharin is added to the electrodeposition solution.

© 2015 The Authors. Published by Elsevier Ltd. This is an open access article under the CC BY-NC-ND license (<http://creativecommons.org/licenses/by-nc-nd/4.0/>).

Peer-review under responsibility of the Scientific Committee of SAM–CONAMET 2014

**Keywords:** Surface treatments; Zn alloys; electrocomposite; coatings; corrosion protection; texture; saccharine; additives

\* Corresponding author. Tel.: +54-11-4-724-6333; fax: +54-11-4-724-6313.

E-mail address: [zulema@inti.gob.ar](mailto:zulema@inti.gob.ar)

## 1. Introduction

The corrosion resistance of zinc (Zn) can be improved by alloying Zn with nickel (Ni), iron or cobalt. ZnNi coatings have high hardness and best decorative Zn properties [Mosavat et al. (2011), Mahmud (2010 tesis)].

The steel sheets coated with ZnNi, particularly those whose composition is about 11-14 % Ni, are widely used in panels of the automobile industry due to its superior corrosion resistance, malleability, weldability, are much better than those of Zn [Espenhahn et al. (1992), Soepenberget al. (1992), Ichida (1995), Fratesi et al. (1996)].

Rajagopalan (1970) and Winand (1994) have reported that alloys containing 20 to 25 % nickel are six times harder than zinc. The codeposition of Ni and Zn was first studied by Schoch and Hirsch (1907) using sulfate solutions with the addition of ammonium sulfate and aluminum sulfate. They remarked the importance to note that the greater the Ni content in the alloy the material resistance against corrosion is higher [Mahmud (2010)].

Beltowska and Lehman (2002) showed that ZnNi electrolyte is stabilized with an additive containing acetate at pH values between 2 and 5.2. An increase of pH leads to a decrease in the nickel content in the coatings for the complexation of acetates, in this case all depends on surface pH and the reaction during the electrolysis.

Byk et al. (2008) have studied the behavior of alloys produced from bath compositions over a wide range. It has been shown that changing the bath composition and the deposition conditions may appear normal or anomalous codeposition of Zn and Ni.

I. Brooks (1998) found that ZnNi alloys hardness could be related to an increase of Ni content in the alloy and it is independent of grain size and texture. Furthermore, the mechanical properties of the material depend stoichiometrically ( $Zn_xNi_y$ ) on its composition. It is known that usually an increase in the thickness involves an increase in resistance to corrosion, was reported by D. Thomas (1984). In this work we have studied the correlation between thickness, texture [Mahmud et al. (2010)] and corrosion resistance [Mahmud et al. (2012)]. Applying independent techniques it was found that the texture changes are related to the thickness of the coating and also to the corrosion resistance in both Zn and in Zn and Ni alloys [Mahmud (2013)]. The study of the microstructure has shown brighter coatings when saccharin is added to the Ni-Zn electrodeposition bath [Park and Szpunar (2000), Oniciu and Muresan (1991), Mahmud et al. (2009)].

## 2. Experimental procedures

The experiments were carried out in a conventional electrolysis cell. The solution was Zn sulphate 1 M and Ni sulphate 1 M in acid media with pH = 3, with alumina or silicon carbide micro particles (2-6  $\mu$ m diameter). Electrodeposition was performed under mechanical agitation to attain higher mass transfer to the cathode. The electrolysis was made by applying a current density of 8 A/dm<sup>2</sup> for different electrolysis times (5-30 min). Finally, we removed the particles attached to the surface by using ultrasound. We have used SEM: scanning electron microscope, EDX: energy dispersive X-ray analysis and optical microscope to observe the cross-sectional area samples of Zn-Ni plus particles on steel included in epoxy resin cured and polished with 600 emery paper. The nickel content and the coating thickness were measured with an X-ray fluorescence (XRF) equipment. Microhardness was quantified with a Leitz Miniload 2. For determining the Zn-Ni hardness, an appropriate load of 25 g was used, which was obtained according to the coatings (from tables). In the texture measurements, the samples were prepared at 8 A/dm<sup>2</sup> with deposition times of 5, 10, 20 and 30 minutes. The measurements were performed with a potentiostat-galvanostat EGG Princeton Applied Research Par 273 and 273 A. Electrochemical Impedance measurements (EIS) were carried out at open circuit potentials in the frequency range from 0.005Hz to 10<sup>5</sup> Hz. The studies of the effect of saccharin as an additive were made by XRD and XRF. For these purposes, the samples were prepared by galvanostatic electrolysis at current density 8 A/dm<sup>2</sup> for 10 min at different saccharine concentrations. The solution of Zn and Ni salts with the addition of micro particles of CSi or micro particles of Al<sub>2</sub>O<sub>3</sub> plus saccharin additive at concentrations  $1.2 \times 10^{-4}$  M to  $5.0 \times 10^{-4}$  M and then the electrolysis with controlled stirring bath along the cathode at room temperature.

### 3. Results and discussions

#### 3.1 Incorporation of particles

The incorporation of a particle into the coating is shown in the area indicated in Fig. 1(a) and its EDX spectrum analysis is shown in Fig. 1(b).

Analysis of Ni % vs J (current density) at different particles concentration, was measured by X-ray fluorescence and the microhardness was measured in a microdurometer (charge: 25 g) and are shown in Fig. 2.

#### 3.2 Nickel content vs J and $Al_2O_3$ concentration. Microhardness vs J and CSi concentration

Fig. 2(a) shows that an increment of the amount of particles into the electrolytic solution produces an increment in the content of Ni in the surface alloy. Likewise, the values of hardness Hv (Vickers) also increase with the increment of the particles concentration in the electrolytic solution, see Fig. 2(b).

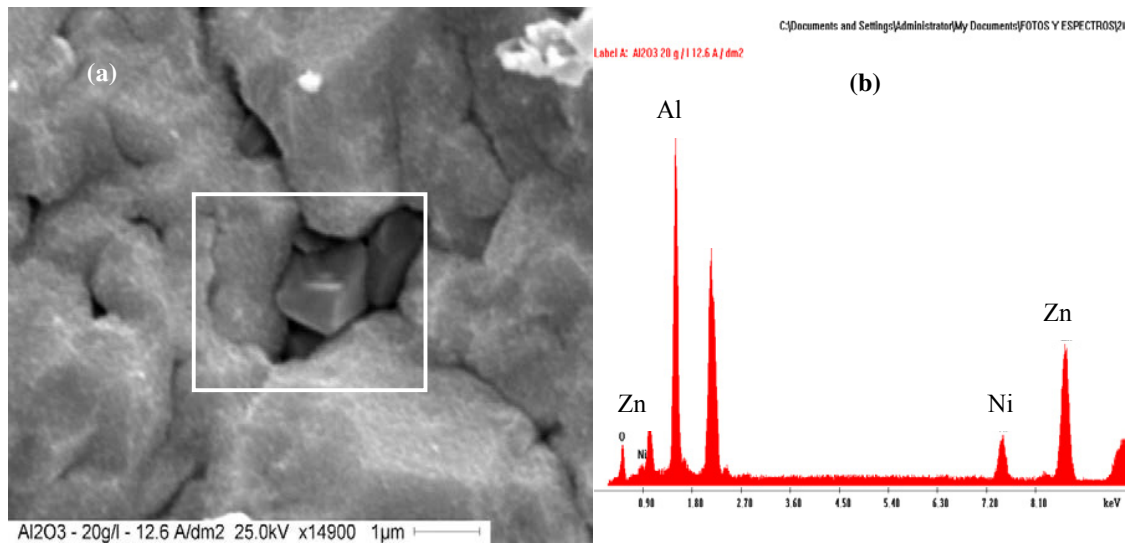


Fig. 1. Photomicrograph by SEM and EDX of ZnNi alloy coatings with (a) alumina particle incorporated; (b) spectrum analysis in a zone of  $20 \mu\text{m} \times 20 \mu\text{m}$ : the elements are Zn, Ni and Al (from alumina) were found in the particle.

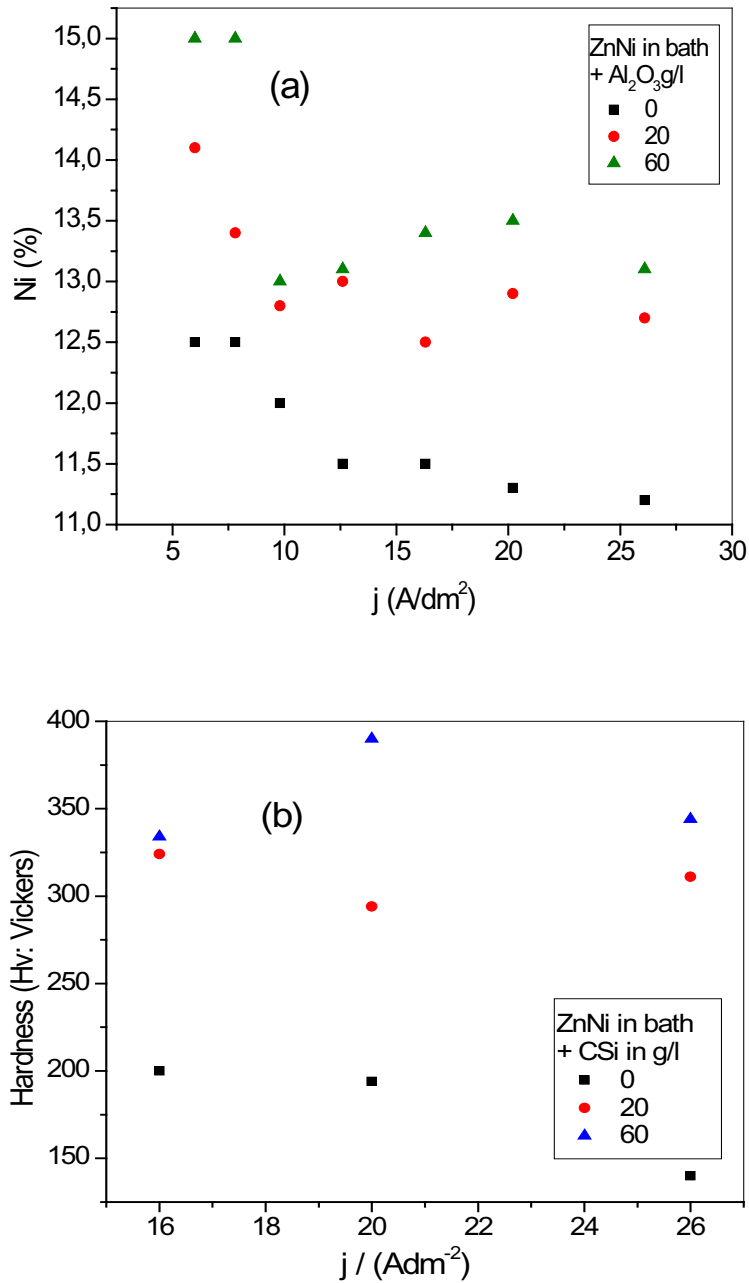


Fig. 2. ZnNi with microparticles: (a) Ni content in ZnNi alloy coating vs j at different Al<sub>2</sub>O<sub>3</sub> concentration in the solution and (b) Microhardness vs j at different CSi concentrations in the solution.

### 3.3 Coating phases and Thickness

We have studied samples with different thicknesses in attention to the importance of choosing a material that resists more drastic conditions in service. We have prepared the specimens at  $J = 8 \text{ A/dm}^2$  because at this current density, the thickness deposited is compatible with industry requirement.

The textures were measured by XRD, and the present phases were determined.

The predominant phases in ZnNi coatings are  $\gamma$  (3,3,0) and Zn (0,0,2) or phase  $\eta$  (1,1,0) for alumina, see Fig. 3. The presence of SiC  $\gamma$  (3,3,0) is reinforced for thicknesses greater than 10 microns (10 minute electrolysis), see Fig. 3(b). In the presence of  $\text{Al}_2\text{O}_3$  a maximum of intensity shows that the alloy crystallizes in phase  $\eta$  (1,1,0), Fig. 3(c). According to XRD analysis the material presents compressive forces, which is an important property in the case where cracks are present in the alloy.

In Fig. 3(b) there is a reinforced intensity vs thickness, at  $10 \mu\text{m}$ , with CSi. In addition, in Fig. 3(c) there is a maximum of intensities in arbitrary unities indicating that a change to phase  $\eta$ (1,1,0) occurs, generating compressive forces. In this case a best material is obtained.

From Fig. 3, we have found an optimum thickness  $10 \mu\text{m}$ , in the presence of microparticles.

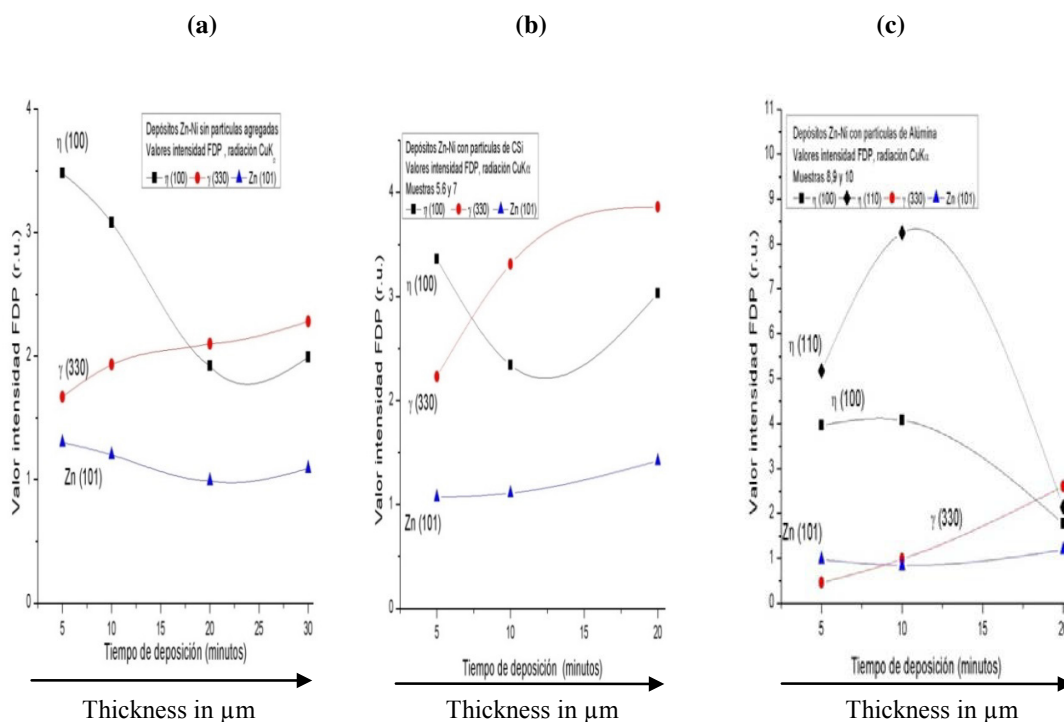


Fig. 3. XRD - FDP "pole figures extracted data from XRD studies". Intensities vs thickness for ZnNi obtained at  $8 \text{ A/dm}^2$  for thickness:  $5 \mu\text{m}$ ,  $10 \mu\text{m}$ ,  $20 \mu\text{m}$ . ZnNi (a) without particles; (b) with CSi 20 g/l; (c) with  $\text{Al}_2\text{O}_3$  20 g/l. In the horizontal axis the time in minutes is proportional to the thickness.

### 3.4 Characterization of ZnNi coatings by EIS and polarization curves

Values of charge transference resistance (RTC) and  $J_0$  were obtained applying EIS and polarization curves. Results for different thickness of coating obtained at  $8 \text{ A/dm}^2$  are shown in Table 1.

Table 1. Characterization of material a  $j = 8 \text{ A/dm}^2$  with several thicknesses  $5 \mu\text{m}$ ,  $10 \mu\text{m}$ , and  $20 \mu\text{m}$ .

ZnNi		EIS- RTC ( $\Omega \text{ cm}^2$ )			Polarization Curve Corrosion Current $J_0$ ( $\mu\text{A/cm}^2$ )		
e / $\mu\text{m}$	Sin part.	CSi	$\text{Al}_2\text{O}_3$	Sin part.	CSi	$\text{Al}_2\text{O}_3$	
5	4000	10000	7000	1,2	20	18	
10	2000	13000	20000	1.9	1.5	1.0	
20	5200	6300	7500	4.0	4.0	1.0	

The RTC values are large for  $10 \mu\text{m}$ , with particles.  $J_0$  corrosion currents are low. In these conditions the material performance is better at the optimum thickness of  $10 \mu\text{m}$ .

### 3.5 The influence of saccharine on the corrosion current $J_0$

Polarization curves in Fig. 4, show that  $J_0$  (corrosion current) increases when the saccharin concentration is increased in the ZnNi+CSi electrodeposition bath. On the other hand there is a shift on the corrosion potential towards negative values.

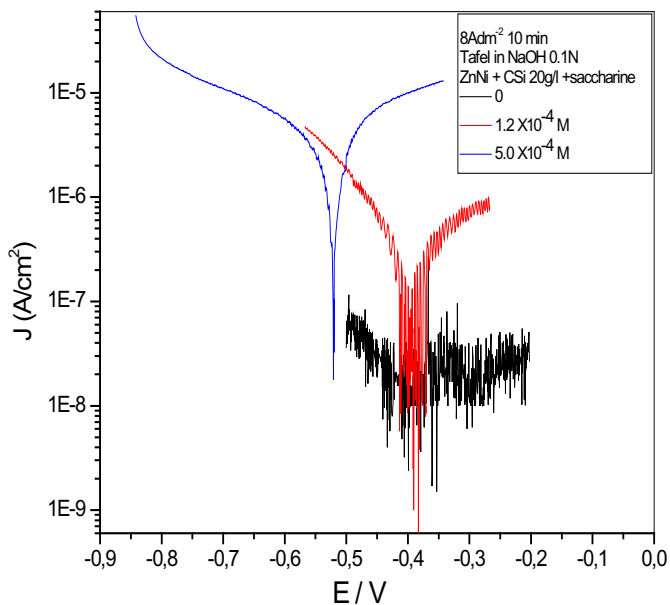


Fig. 4. Polarization curves ZnNi + CSi (a) without saccharine, (b) with  $1 \times 10^{-4}$  M saccharine, (c) with  $5 \times 10^{-4}$  M saccharine in Na OH 0.1 N with buffer boric borate, pH 9.2. Scan rate  $v = 1 \text{ mV/s}$ .

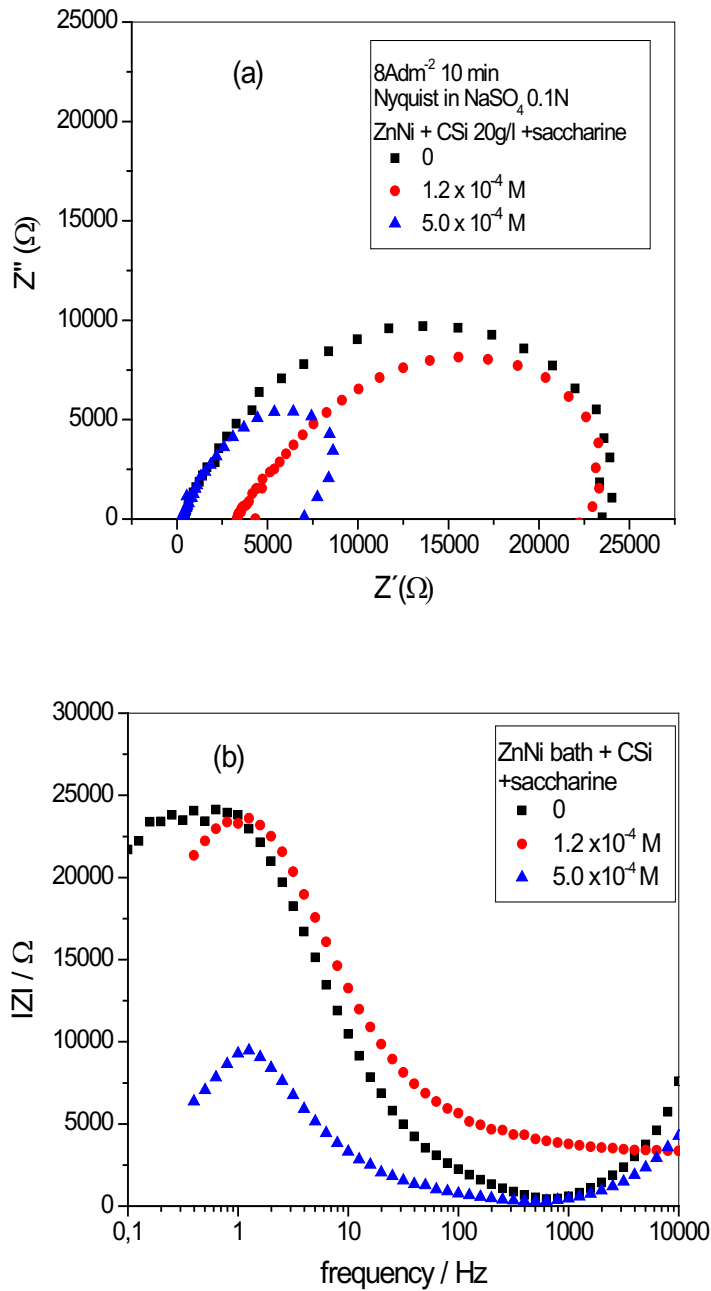


Fig. 5. EIS curves obtained in  $\text{Na}_2\text{SO}_4$  0.1 M, pH 6.0. Scan from 100 KHz to 5 mHz. ZnNi +CSi (20 g/l) + saccharine: 0 (squares),  $1.2 \times 10^{-4}$  M saccharine (circles),  $5.0 \times 10^{-4}$  M saccharine (triangles). (a) Nyquist Diagram  $Z''$  (imaginary component) vs  $Z'$  (real component); (b) Bode Diagram  $|Z|$  vs. frequency.

Coatings obtained using solutions without saccharine show the same RTC value of those produced from solutions with a concentration  $10^{-4}$  M of this additive, but in the last case with a better microstructure and reduced crystal size.

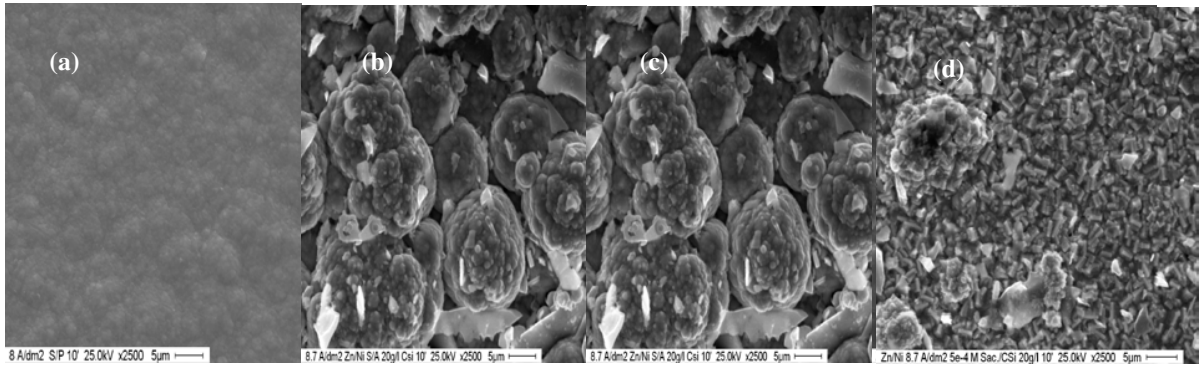


Fig. 6. Photomicrograph obtained by SEM in ZnNi coatings obtained at 8 A/dm<sup>2</sup> 10 min (a) without particles, (b) with CSi, (c) with CSi +  $1.2 \times 10^{-4}$  M and (d) with CSi +  $5.0 \times 10^{-4}$  M.

Fig. 7. shows that the Ni content decreased as the saccharin concentration increased to  $5.0 \times 10^{-4}$  M.

### 3.6 X-ray diffraction

XRD studies, presented in Fig. 8, show the intensities of the phases obtained in the deposition conditions at variable J values for a deposition time of 10 min. It is known that in the ZnNi the  $\gamma$  (3,3,0) phase is always present with varying intensity and depends on the coating.

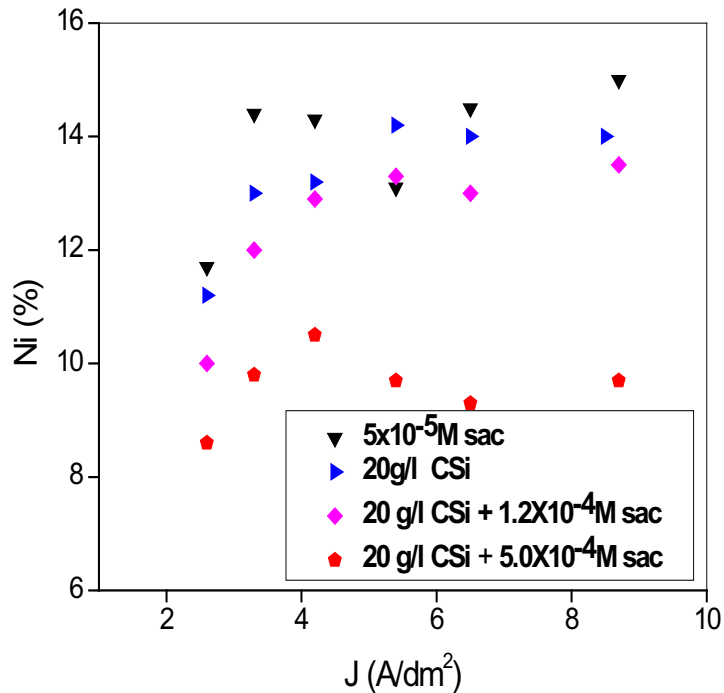


Fig. 7. Ni (%) vs J for different ZnNi compositions in the bath. black  $5 \times 10^{-5}$  M saccharine, blue CSi 20 g/l, pink CSi 20 g/l +  $1.2 \times 10^{-4}$  M, red CSi 20g/l +  $5.0 \times 10^{-4}$  M.



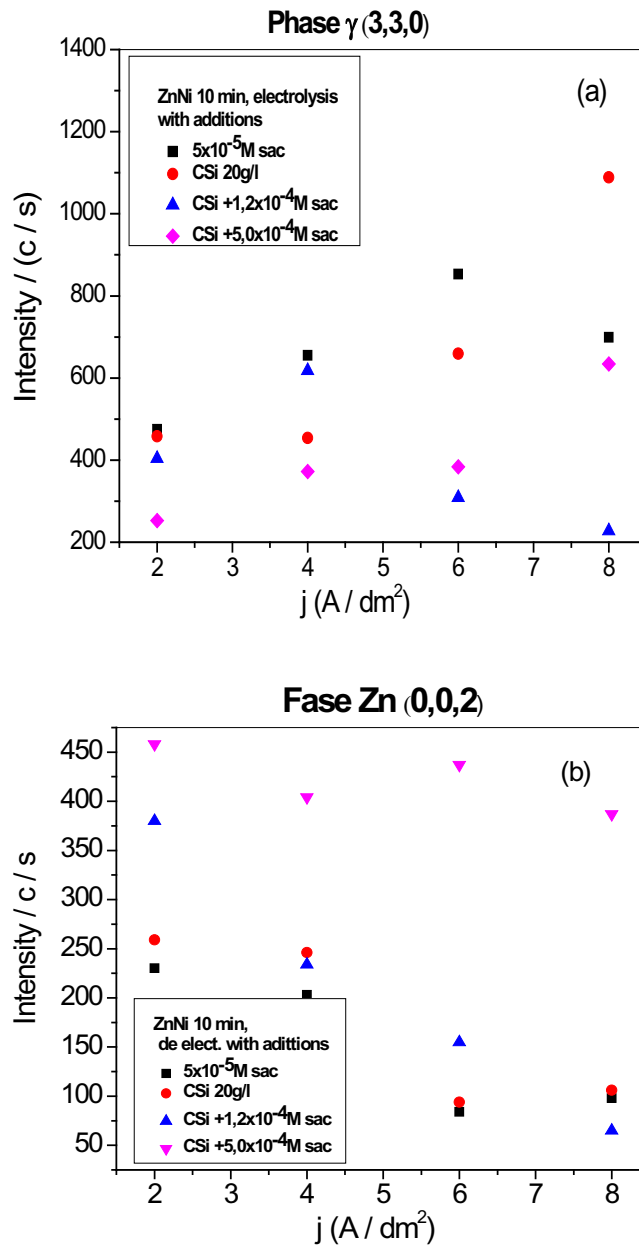


Fig. 8. Intensities of present phases in the ZnNi coatings with CSi microparticles and saccharine I vs  $j$  (A/dm<sup>2</sup>). (a) phase (3,3,0); (b) phase Zn (0,0,2).

The ZnNi phase Zn (0,0,2) seen in Fig. 8(b) shows that ZnNi in the presence of SiC and saccharin ( $5 \times 10^{-4} \text{M}$ ) has high intensity at all current densities studied.

This is due to the high binding energy of the atoms on the surface and the total energy involved in the structure. In these conditions the material is electrochemically less active.

#### 4. Conclusion

- Alumina or silicon carbide particles incorporated in the Ni-Zn coating modify the corrosion resistance of the material. This is because the presence of alumina or SiC particles increases the percentage of Ni in the alloy.
- The hardness of the material increases in the presence of both types of particles in the Ni-Zn. The material thickness influences the quality of the material.
- There is an optimum thickness of 10  $\mu\text{m}$  in which ZnNi with CSi reinforces  $\gamma$  (3,3,0) textures and changes to  $\eta$ (1,1,0) phase in ZnNi with  $\text{Al}_2\text{O}_3$ .
- The analysis of operation variables to obtain the material has shown that using a current density electrolysis of 8  $\text{A}/\text{dm}^2$  for 10 minutes and an adequate concentration in the component of bath and controlled stirring a material with better barrier properties and microstructure is achieved in the presence of particles and saccharine additive.

#### References

- Beltowska and Lehman., 2002. Surface and Coating Technology 151-152, 444.
- Byk, T. V. Gaevskaya, and L. S. Tsybulskaya., 2008. Effect of electrodeposition conditions on the composition, microstructure, and corrosion resistance of Zn–Ni alloy coatings. *Surf. Coatings Technol.*, vol. 202, no. 24, pp. 5817–5823.
- Brooks, I. 1998. Thesis. Characterization of Nanocrystalline Single.
- Douglas Thomas ; 1985. Corrosion Test”, *Electroplating Engineering Handbook*. Durney, L.J. 4th ed. 328.
- Espenhahn, M., 1992. 2nd International Conference on Zinc and Zinc Alloy Coated Steel Sheet; *Galvatech* 92,273.
- Fratesi, R. Roventi, G.,1996. Corrosion resistance of Zn-Ni alloy coatings in industrial production, vol. 82, pp. 158–164.
- Ichida, T., 1995. 3rd International Conference on Zinc and Zinc Alloy Coated Steel Sheet; *Galvatech* 95, 359.
- Mahmud, Z., 2009. Efecto de los aditivos en el desempeño de los recubrimientos de ZnNi. *SAM. Asoc. Argentina Mater. Regist. N° ISSN 1668-4788*, vol. 6 N° 1, pp. 5–11.
- Mahmud, Z., 2010. Influencia de los aditivos utilizados en el cincado en medio ácido. Thesis. Universidad de Buenos Aires, FCEN-UBA. pp323.
- Mahmud, Z. A. Pina, J. Mingolo N. Gassa, L. Gordillo, J. 2010. RECUBRIMIENTO CONSTITUÍDO DE UNA ALEACIÓN DE ZnNi MÁS PARTÍCULAS CERÁMICAS DE CARBURO DE SILICIO Ó ALÚMINA. In *Encuentro de Primavera INTI*.
- Mahmud, Z., 2011. Efecto del agregado de alúmina en la calidad del recubrimiento de aleación de Zinc Níquel in *Congreso Internacional de Materiales- CIM – Colombia*.
- Mahmud Z. Paulo T. Gordillo, J. M. N. 2012. Efecto del agregado de partículas cerámicas en la composición de la aleación de Zinc Níquel. In *XX Congreso da Sociedade Iberoamericana de Electroquímica* (pp. 2–3).
- Mahmud, Z., 2013. New material comprising a Zn metal matrix and ceramic particles having very good mechanical properties and high corrosion resistance Alumina incorporated steel, in *EUROMAT 2013- European Congress and Exhibition on Materials in Sevilla-2013*.
- Mosavat, S H, Bahrololoom, M E, Shariat, M H. 2011. Applied Surface Science Electrodeposition of nanocrystalline Zn – Ni alloy from alkaline glycinate bath containing saccharin as additive. *Applied Surface Science*, Vol 257- 8311-8316.
- Oniciu, L., Muresan, L., 1991. Some fundamental aspects of levelling and brightening in metal electrodeposition. *Journal of Applied Electrochemistry* 21-565-574.
- Park and Szpunar. 2000. The microstructural characterization of electrogalvanized zinc-iron and zinc- nickel coatings. *Textures and Microstructures*, Vol. 34. pp. 119-146. Printed in Malaysia.
- Rajagopalan., S.1970. Metal Finishing Vol70- pp52.
- Schoch , A., 1907. *J.Am. Soc.*, 29- 311.
- Soepenber, E., 1992. 2nd International Conference on Zinc and Zinc Alloy Coated Steel Sheet; *Galvatech* 92, 278.
- Winand, R. 1994. Electrodeposition of metals and alloys—new results and perspectives. *Electrochimica Acta*. doi:10.1016/0013-4686(94)E0023-S.